

FLEXURAL BEHAVIOR OF NORMAL AND HIGH STRENGTH CONTINUOUS BEAMS REINFORCED BY GFRP BARS

Muayad M. Abdullah¹

*Hassan F. Hassan¹

1) Civil Engineering Department, Mustansiriyah University, Baghdad, Iraq

Received 5/7/2020

Accepted in revised form 23/8/2020

Published 1/1/2021

Abstract: In the reinforced concrete structures, fiber reinforced polymer (FRP) has been considered an alternative material to steel reinforcement with the advantages of corrosion resistance, non-conductivity, and high strength to weight ratio. This work is devoted to study the flexural behavior of normal and high strength concrete continuous beams reinforced with glass fiber reinforced polymers (GFRP) bars. Ten continuous beams, with dimensions 150 mm wide × 250 mm deep × 2300 mm long consisting of two equal spans were investigated in this study. The beams were divided into three groups according to the compressive strength of concrete (30, 50 and 70) MPa. Each group consists of three beams with different longitudinal reinforcement ratio (ρ_{fmin} , ρ_{fb} and $1.5\rho_{fb}$; where ρ_{fmin} and ρ_{fb} are the reinforcement ratio at a minimum and balanced condition, respectively). The ultimate load, mid-span deflection, cracks size, concrete strains, GFRP reinforcement strains of the tested beams were verified and contrasted. The experimental results indicate that the increase in the longitudinal reinforcement ratio increases the ultimate load by 125% and decreases the crack size and mid-span deflection by 78% and 57%, respectively. The experimental data were compared with the proposed ACI 440.1R-15 and CSA S806-12 equations. the ultimate load were greater than the calculated results according to (ACI 440.1R-15) by (20%) for beams with (ρ_{min}), while beams with (ρ_b and $1.5\rho_b$) the ultimate load were less than the calculated results by (9%), cracks size were close to the results according to (ACI 440.1R-15) for normal strength beams, while for high strength beams results were less than the results according to (ACI 440.1R-15), while ISIS-Canada 07 showed good agreement for all tested beams..

Keywords: *Flexural Behavior, Continuous Beams, GFRP Bars, Crack Size, Ductility.*

1. Introduction

Decades of studies and practical use have allowed fiber-reinforced polymers (FRPs) to become a particularly effective steel substitute while avoiding corrosion problems due to their different advantages compared to the conventional materials like high tensile strength, low self-weight, ease of use, easy maintenance and even in rather harsh environments high durability [1-3]. Carbon, glass, and aramid are the most common types of fibers. GFRP bars have a linear stress-strain relationship under stress up to collapse; although they have lower elasticity modules and no ductility such as steel bars, GFRP bars were used in a developing number of applications due to their higher performance at a reasonably competitive cost [4-7].

The flexural behavior of simply supported concrete members reinforced with FRP bars experimentally studied by a several of studies, Barris et al. [8] tested twelve simply supported

* Corresponding Author: hassanfala@gmail.com

beams reinforced by GFRP bars, the main variables were longitudinal reinforcement ratios and effective depth-to-height ratios, all beams demonstrated a concrete crushing mode of failure with ultimate load 51% than expected according to ACI 440.1R-06 [9], also a High degree of deformability was attained before failure. Yinghao and Yong [10] studied the flexural behavior of high strength simply supported concrete beams reinforced with hybrid steel reinforcements and (GFRP), the arrangement of reinforcement layers was the main parameters considered, the use of reinforcement bars (GFRP - Steel) in the form of a single layer is more effect on ultimate moment capacity than the other arrangements, deflection and cracks size of hybrid beams is greatly affected by the depth of the steel layer. Adam et al. [11] presented an experimental and theoretical study of the flexural behavior of concrete beams reinforced with locally produced (GFRP) bars, the main parameters were reinforcement material type (GFRP and steel), concrete compressive strength and reinforcement ratio, the test results showed that, by increasing the reinforcement ratio, the crack sizes and mid-span deflection were reduced significantly, the final load for over-reinforced sections increased by 97% as compared with balanced section and ACI 440.1R-06[9] codes showed underestimate deflection values of FRP reinforced concrete beams. Maranan et al. [12] evaluated the flexural strength of geopolymer concrete beams reinforced with (GFRP) bars; the parameters analyzed were nominal bar diameter, reinforcement ratio, and anchorage method. Based on the experimental results, the bar diameter did not have a significant effect on the flexural efficiency of the beams and the efficiency of the beam is improved as the reinforcement ratio increases. Yang et al. [13] presented the entire destruction growth progression in the form of crack destruction and

energy dissipation of concrete beams reinforced with (GFRP) bars, they concluded that the advanced FE model developed is appropriate as a feasible and economical method for accurate modeling and analysis of the damage behavior of concrete beams reinforced with GFRP bars, in particular in design-oriented parametric studies. Dong et al. [14] investigated the flexural performance of concrete beams reinforced with FRP bars grouted in corrugated sleeves test results showed that the use of FRP bars grouted in corrugated sleeves in beam tension zone was an effective method to reduce crack sizes and improving performance in serviceability, and Reinforced FRP beams at the beginning of concrete crushing showed greater deflection than the steel-RC beam. FRP reinforced beams may also give a sign of failure by experiencing significant cracking and large deflection. Ahmed et al. [15] studied Flexural strength and failure of geopolymer simply supported concrete beams reinforced with CFRP bars, results showed The reinforcement ratio affected the rigidity of the beam specimens. As a result, the beams with a low reinforcement ratio were significantly deformed and the final load increase (17.5–155.8 %) was recorded with an increasing reinforcement ratio as regards their load-deflection behavior.

There are limited studies on the behavior of continuous beams reinforced with FRP bars, the main objective of the study carried out by Tezuka et al. [16] on a continuous beam consisting of two spans, The studied variables were reinforcement material (Aramid FRP, Carbon FRP and steel prestressing wires), and prestressing level of reinforcement (with or without prestressing), It has been found that the calculated curvature appears to be greater than the experimental curvature because the stiffness of the section at the middle support is underestimated. The behavior and ductility on

continuous beams reinforced with different types of FRP were experimentally studied by Grace et al. [17], the reinforcement types used were steel, CFRP and GFRP bars test results indicated that the use of GFRP stirrups increased shear deformation and deflection, the use of GFRP bars altered the pattern of failure from bending to shear or shear bending depending on the longitudinal reinforced used, Continuous beams reinforced by FRP experienced a greater deflection compared to their counterparts reinforced with steel. Habeeb and Ashour [18] conducted an experimental research on continuous concrete beam reinforced with (GFRP) longitudinal bars; the major parameter investigated was the amount of GFRP reinforcement, The experimental results indicate that the over-reinforcement of the bottom layer of continuously supported GFRP beams is a main factor in monitoring the size and propagation of cracks, increasing the ultimate load and decreasing the deflection of these kind of beams. Zinkaah and Ashour [19] experimentally tested to failure nine continuous concrete deep beams reinforced with (GFRP) bars, the main parameters were evaluated: the span-to-overall depth ratio of the shear, web reinforcement and the size effect, the test results were used to assess the applicability of the methods suggested by the American, European, and Canadian codes as well as previous studies to predict the load capacity of continuous deep beams reinforced with GFRP bars. Mohamed et al. [20] examined the behavior of simple and continuous concrete deep beams reinforced with GFRP bars, the test parameter was the shear span-to-depth ratio, results showed that the ACI 318-14 code [21] for steel-RC structures was un-conservative in calculating GFRP-RC capacity of simple and continuous beams; where the experimental load capacity was lower than the calculated ones, with an average of (0.59 and 0.75) %, respectively. Abdallah et al. [22]

studied the strengthening of continuous reinforced concrete (RC) beams with CFRP and GFRP bars by using the Near Surface Mounted (NSM) technique, the major test parameters were the type, ratio and length of the FRP bars and the filling material properties, the test results showed that the moment of redistribution and ductility of the (NSM-FRP) beams were adversely affected by increased FRP reinforcement, decreased FRP length or the use of mortar as a filler material rather than epoxy resin..

2. Research Significance

Complementary to previous research on the flexural behavior continuous beams reinforced with FRP bars, this research provides a study on the behavior of this type of beams taking in consideration the increase in concrete compressive strength and the ratio of longitudinal GFRP reinforcement also includes a study of the effect of this type of reinforcement on the failure characteristics of beams like deflection, the size of cracks, modes of failure and ductility and comparison the experimental results with the American , Canadian code and some proposed equations from the previous research

3. Experimental Program

3.1 Materials

3.1.1 Concrete

The concrete mixture made of cement, sand, coarse aggregate size with 10mm nominal max size, superplasticizer, micro silica and water, Table 1 shows the mix proportions of concrete used in this study.

3.1.2 GFRP Bars

GFRP bars used in this study were produced NANJING FINGHUI ® _China [23]; bars were contrived by the pultrusion method of E-glass fibers impregnated in modified vinyl ester resin.

Table 1. Mix proportion of concrete

"Mix"	"G (kg/m3)"	"S (kg/m3)"	"C (kg/m3)"	"SP %"	MS(kg/m3)	W/C
N	1000	550	400	0	0	0.45
H1	767	880	575	4	45	0.3
H2	500	900	650	4	90	0.22

G: coarse aggregate , S: sand, C: cement; SP: superplasticizer is % of the weight of cement; MS: micro silica, W/C: water-cement ratio.

Table (2) provides the results of the tensile tests carried out on samples of the used GFRP bars, tensile and modulus properties were calculated in accordance with ASTM Standard (ASTM D7205-06) [24].

Table 2. GFRP bars specifications

Bar type	GFRP
Density (G/cm3)	2.2
Ultimate strength (MPa)	1200
Modulus of elasticity (MPa)	55000
Strain, ϵ_{fu} ($\mu\epsilon$)	1950

3.2 Details of tested beams

The design methods defined according to the ACI 440.1R-15 [25] and ACI 318R-14 [21] were followed for design nine continuous beams reinforced with GFRP bars

and one reference beam reinforced with conventional steel, respectively. The beams were distributed into three groups depending on the concrete compressive strength. Each group consists of three specimens with different GFRP reinforcement ratio (ρ_{fmin} , ρ_{fb} and $1.5 \rho_{fb}$), with a adequate quantity of shear reinforcement to fail either due to tensile failure due to GFRP bar fracturing or crushing of concrete in the central region, examined beams specifics are summed up in Table 3

The specimens were measured with an effective range of 1100 mm for each span subjected to 2-point loading at mid of each span, all beam with rectangular section with (250×150) mm dimensions, each specimen was supported roller Support assemblies and sharp edges to allow for movement and turning. Configuration of the test is outlined in Fig. 1

Table 3. Specifics of tested beams

Beam mixture type	Beam specimen	Target concrete strength(MPa)	Bottom reinforcements (GFRP bars) Φ in mm	Top reinforcements (GFRP bars) Φ in mm	Stirrups ^b (steel bars)
N	"BS-30-2"	30	1 ϕ 6+2 ϕ 10 ^a	2 ϕ 8	8@100
	"BG-30-1"	30	4 ϕ 6	2 ϕ 8	8@100
	"BG-30-2"	30	1 ϕ 6+2 ϕ 10	2 ϕ 8	8@100
	"BG-30-3"	30	1 ϕ 10+2 ϕ 13	2 ϕ 8	8@100
H1	"BG-50-1"	50	2 ϕ 10	2 ϕ 8	8@100
	"BG-50-2"	50	3 ϕ 13	2 ϕ 8	8@100
	"BG-50-3"	50	1 ϕ 10+3 ϕ 13	2 ϕ 8	8@100
H2	"BG-70-1"	70	1 ϕ 6+2 ϕ 10	2 Φ 8	8@100
	"BG-70-2"	70	2 ϕ 16	2 ϕ 8	8@100
	"BG-70-3"	70	3 ϕ 16	2 ϕ 8	8@100

^a reference beam reinforced with steel bars

^b the stirrups spacing were 100mm along the beam except interior support region were 50mm due to high shear stress

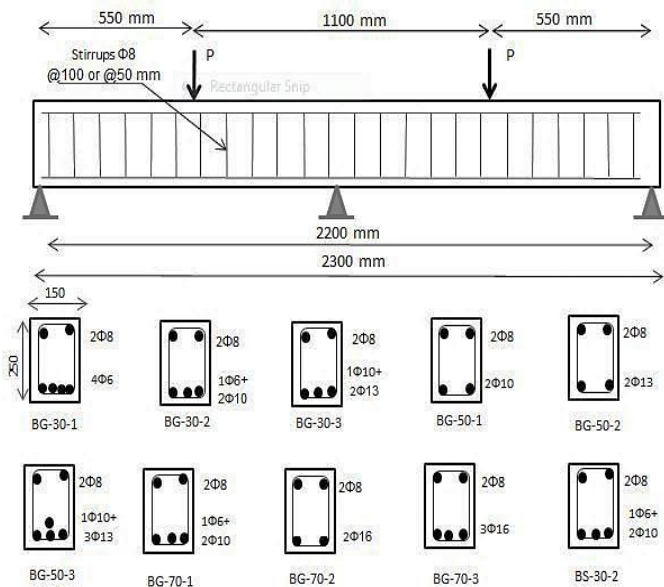


Figure 1. Tested beams geometry and details.

4. Test Results And Discussion

This division summarizes the tests data, containing the load–deflection performance, collapse type, flexural strength, central deflection, strains concrete, GFRP strain, crack size, number of cracks and crack performance of beams experienced.

4.1. Load-deflection performance

The experimental load of the GFRP reinforced concrete continuous beams to central deflection and collapse loads were shown in Figures 2 to 4. The curve matches the central beam deflection readings obtained from the dial gage. Visually examined during the test beams appear up to the first crack, and the load value corresponds was recorded. The first cracking load was also checked from the load- deflection figures and concrete tensile strain. Table 4 summarizes the main findings for all experiments beams.

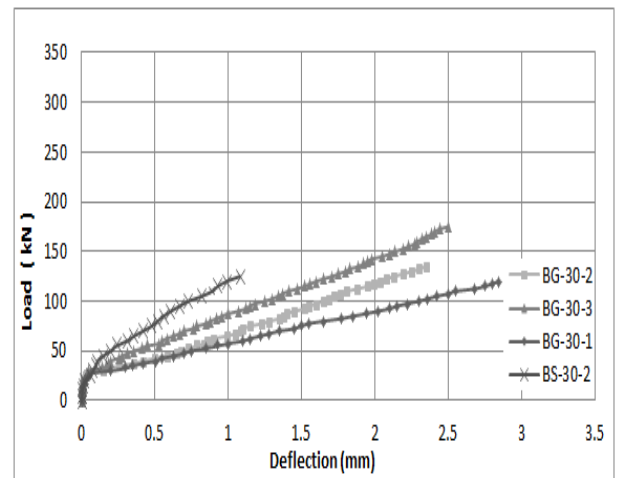


Figure 2. Load–midspan deflection of beam with $f'c=30$ MPa

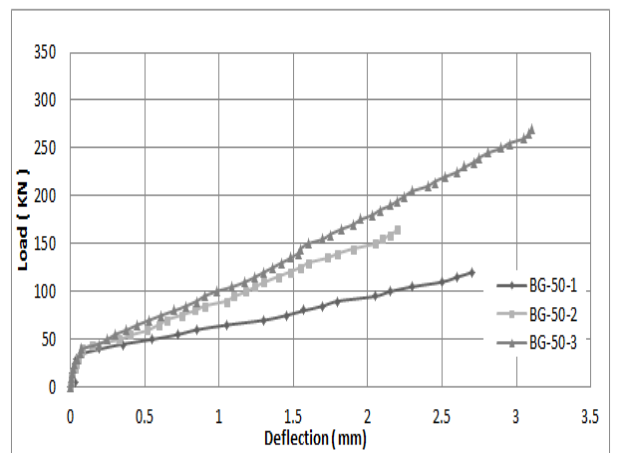


Figure 3. Load–midspan deflection of beam with $f'c=50$ MPa

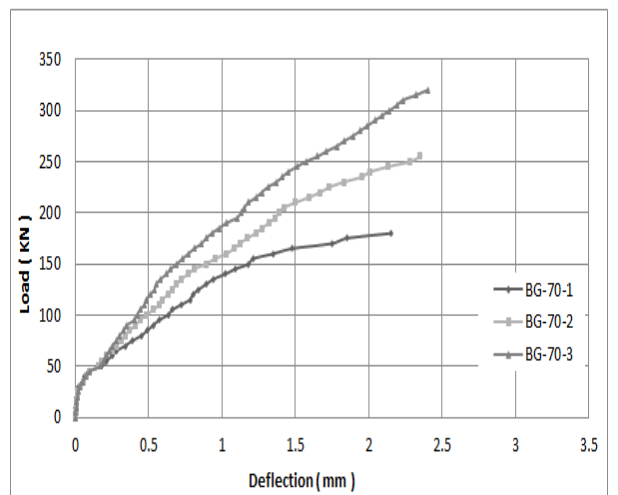


Figure 4. Load–midspan deflection of beam with $f'c=70$ MPa

Table 4. Experiments results and modes of failure

Beam specimen	Reinforcements Ratio (%)	$f'c$ (MPa)	"Initial cracking load, Pcr (kN)"	"Failure load, Pu,exp (kN)"	Pcr / Pu,exp	Maximum midspan deflection (mm)	Collapse modes a
"BG-30-1"	0.00383 b	31.5	29	119.5	0.24	2.8	G.R
"BG-30-2"	0.00529 c		30.2	135.5	0.22	2.35	G.R+ C.C
"BG-30-3"	0.00984 d		32	176	0.18	2.5	C.C
"BG-50-1"	0.00433 b	50.75	38	125	0.3	2.65	G.R
"BG-50-2"	0.00767 c		41.4	166	0.24	2.25	G.R+ C.C
"BG-50-3"	0.0136 d		42	270	0.15	3.1	C.C
"BG-70-1"	0.00529 b	71.5	47	180	0.26	2.2	G.R
"BG-70-2"	0.012 c		48	256	0.18	2.35	G.R+ C.C
"BG-70-3"	0.01797 d		50.1	325	0.15	2.4	C.C
BS-30-2	0.00529 e	31.5	34.5	125	0.27	1.08	S.R

a C.C: crushing of concrete, G.R: GFRP bars rupture, Steel bars rupture.

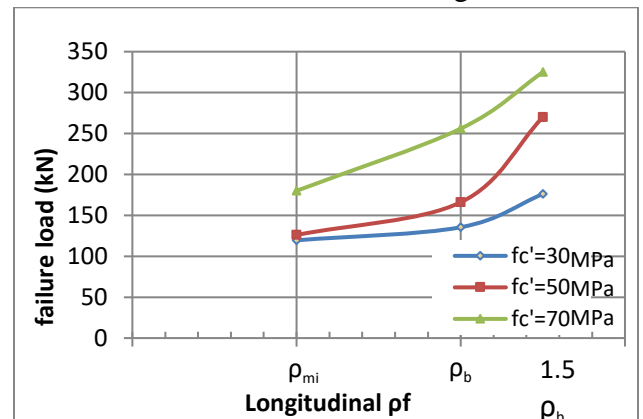
b Minimum reinforcement ratio (ρ_{fmin}) **c** Balanced reinforcement ratio (ρ_{fb}) **d** (1.5 ρ_{fb})

e Reference beam reinforced by steel bars

4.1.1 Effect of reinforcement ratio

Table 5 and Figure 5 illustrations the reinforcement ratio influence on the failure load, it can be gotten that the increase in (ρ_f) increase the failure load, increasing the (ρ_f) from (ρ_{fmin}) to (ρ_{fb}) lead to increase the failure load by (13, 38 and 42%) for beams with compressive strength (30, 50 and 70 MPa), respectively. While the increase in failure load when (ρ_f) increasing from (ρ_{fmin}) to (1.5 ρ_{fb}) were (47, 125 and 80%) for the same order of concrete compressive strength, it can be noticed that the percentage of increase in failure load was slight in normal strength concrete beams while this Percentage was significant for high strength

concrete beams . The increasing in (ρ_f) decreases the deflection at the same load level for all tested beams as shows in Figures 2 to 4.

**Figure 5.** Effect of reinforcement ratio on failure loads**Table 5.** Effect of reinforcement ratio on failure loads

Beam specimen	$f'c$ (MPa)	Reinforcements ratio (%)	Failure load, Pu (kN)	Increasing ratio of Pu (%)
"BG-30-1"	31.5	0.383 a	119.5	0
"BG-30-2"		0.529 b	135.5	13
"BG-30-3"		0.984 c	176	47
"BG-50-1"	50.75	0.433 a	125	0
"BG-50-2"		0.767 b	166	32
"BG-50-3"		1.36 c	270	116
"BG-70-1"	71.5	0.529 a	180	0
"BG-70-2"		0.012 b	256	42
"BG-70-3"		0.01797 c	325	81

a Minimum reinforcement ratio (ρ_{fmin}) **b** Balanced reinforcement ratio (ρ_{fb}) **c** (1.5 ρ_{fb})

4.1.2 Concrete compressive strength efficiency

The examined beams with the same dimensions and reinforcement area would differ only in f'_c , BG-30-2 and BG-70-1. By increasing the concrete compressive strength, the deflection in the same consequent load levels was reduced. The ultimate load increased by 32.8% when concrete compressive strength increased from 31.5 to 71.5 MPa. The compressive strength had a major influence on the first crack, particularly when the f'_c increased from 31.5 MPa to 71.5 Mpa, where the first load of cracking increased 55.6%.

4.2 Mode of failure

As shown previously Table 4 summarizes the modes of failure found for the beams tested. The most common mode of failure was concrete crushing for all over reinforced beams (beams reinforced with (1.5 ρ_{fb})), whereas all beams reinforced with (ρ_{fmin}) failed by rupture of GFRP bars. On the other hand the compound failure mode (crushing of concrete and GFRP bars rupture) was seen in all balanced reinforced sections. The ACI 440.1R-15 [25] and CSA S806-12 [26] codes recommend crushing concrete failure for any concrete beams reinforced with FRP bars meanwhile this type of failure is less brittle, further gradual, and less disastrous with higher deformability related to the rupture of FRP bars [27,28]. In addition, more shear

cracks appeared and propagated intensely for beam specimens with a higher GFRP reinforcement ratio. This can be attributed to the greater shear stress relating to the higher final load. Figure 5 shows modes of failure of the tested beams.

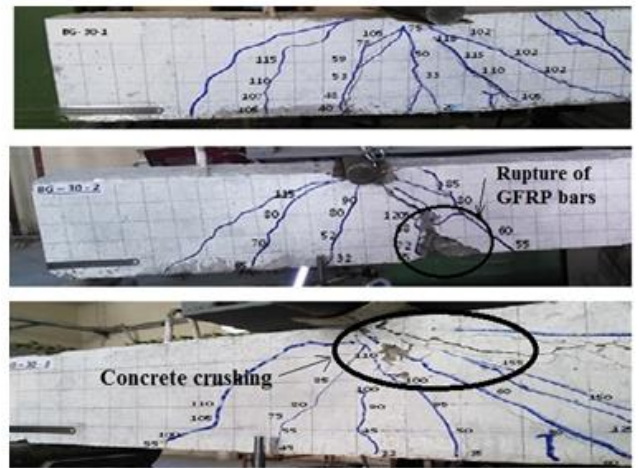


Figure 5. Failure modes of tested beams

4.3 Load-strain relationships

4.3.1 GFRP strain

Figures 6 to 8 presents the load – GFRP strain relationship for all tested beams, increasing in GFRP reinforcement ratio decreases the strain in bars, at the same load level ($P=119.5kN$) for beams with ($f'_c =30$) MPa the strain in the (GFRP) bar decreased by (31 and 53%) when the reinforcement ratio increased from (ρ_{fmin}) to (ρ_{fb} and 1.5 ρ_{fb}), respectively. While for beams with ($f'_c =50$) MPa at a load of (125kN) the strain in the (GFRP) bars decreased by (61 and 72%) as the reinforcement ratio increased from (ρ_{fmin}) to (ρ_{fb} and 1.5 ρ_{fb}), respectively. In addition for beams with ($f'_c =70$) MPa at a load of (180kN) GFRP bars strain decreased by (57 and 78%) as the reinforcement ratio increased from (ρ_{fmin}) to (ρ_{fb} and 1.5 ρ_{fb}), respectively. From the above results it can notice that the increasing in concrete compressive strength increases the decreasing percentage in GFRP bars strain, also for beams with the same reinforcement area BG-30-2 and BG-70-1 increasing the concrete compressive strength from 31.5 to 71.5 MPa decreased the GFRP strain by 32.4%.

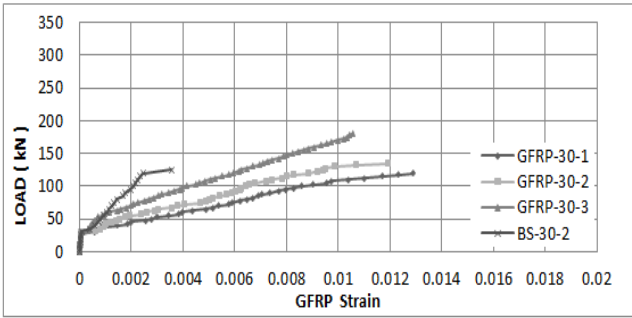


Figure 6. Load–GFRP strain of beam with $f'_c=30$ MPa

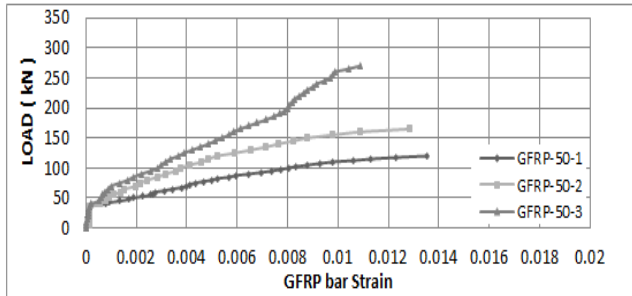


Figure 7. Load–GFRP strain of beam with $f'_c=50$ MPa

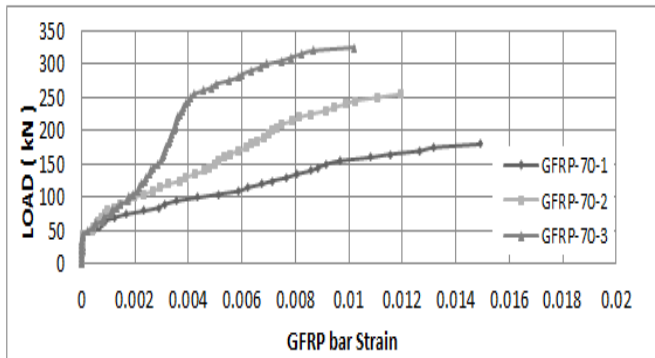


Figure 8. Load–GFRP strain of beam with $f'_c=70$ MPa

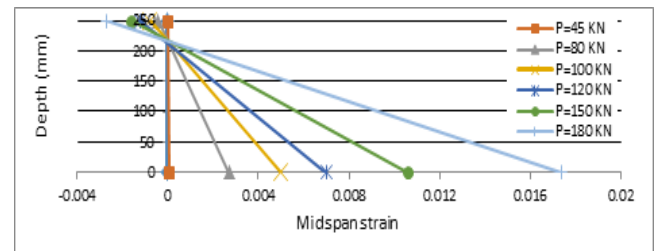
4.3.2 Concrete strain and neutral axis depth

The data provided by the two electrical strain gauges on the concrete surface at the extreme top and bottom ends of the mid-span section showed that the maximum compressive strain ϵ_{cu} between 0.25% and 0.33% , these values were match with one established by the ACI440.1R-15 [25] which consider ϵ_{cu} to be between 0.3% and 0.35%.

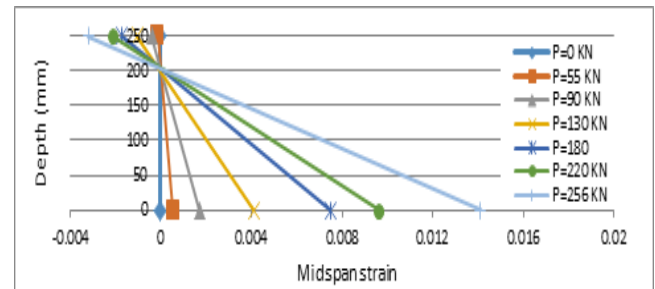
The position of the neutral axis (N.A) depth of the critical sections increases with the increase of the ratio of longitudinal reinforcement ratio from (ρ_{fmin}) to ($1.5 \rho_{fb}$) for all tested beams. This

behavior is due to the increase in the tensile strength resulting from the increase in the ratio of reinforcement, which leads to an increase in the equivalent compressive strength and, consequently, to an increase in the compressive area. However, the effect of concrete strength on the depth of the neutral axis (N.A) is very little or insignificant. Figure 9 shows concrete strain development along the midspan depth of some tested beams.

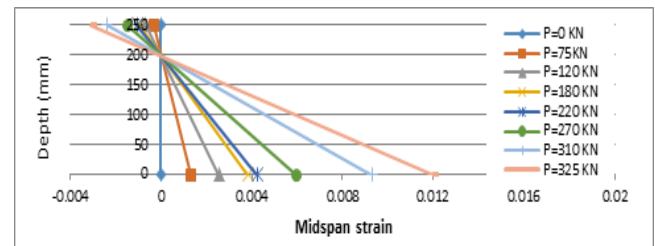
Specimens having higher f'_c can be possessed higher (N.A.) depths. These remarks were close with the common formulation to compute the (N.A.) position in the serviceability conditions for sections without compression reinforcement.



A-BG-70-1



B-BG-70-2



C-BG-70-3

Figure 9. Concrete strain distribution at midspan depth

4.4 Crack size

The cracks size are measured using image analyzed using Photoshop Creative Cloud (CC) software where a real scale object reference is located at the same distance of tested beam and then the captured image analyzed for crack size prediction with high accuracy. Figures 10 to 12 shows the relationship between the cracks size (W_{cr}) in the mid-span and the load applied on each beam, the first cracks appeared at the internal support due to the fact that the shear strength and the amount of bending moment are greater in this region than the rest of the critical sections in continuous beam.

The increasing (ρ_f) leads to minimize the size of crack. At a load of (60 kN), the crack size noted values of, (0.43 mm, 0.35 and 0.3 mm) for beam (BG-30-1, BG-30-2 and BG-30-3), respectively. While, at a load of (100 kN) the size of crack is (1.3 mm, 0.6 mm, and 0.3 mm) for beam (BG-50-1, BG-50-2 and BG-50-3) respectively. In addition, at a load of (150 kN) the crack size noted values of (0.94 mm, 0.52 mm and 0.3 mm) for beam (BG-70-1, BG-70-2 and BG-70-3), respectively, results showed that there was a significant decrease in crack size due to increasing in reinforcement ratio for beams with $f'_c = 50$ and 70 MPa than beams with $f'_c = 30$ MPa, also for beams with the same reinforcement area BG-30-2 and BG-70-1, increasing the concrete compressive strength from 31.5 to 71.5 MPa decreased the crack size by 48.6%.

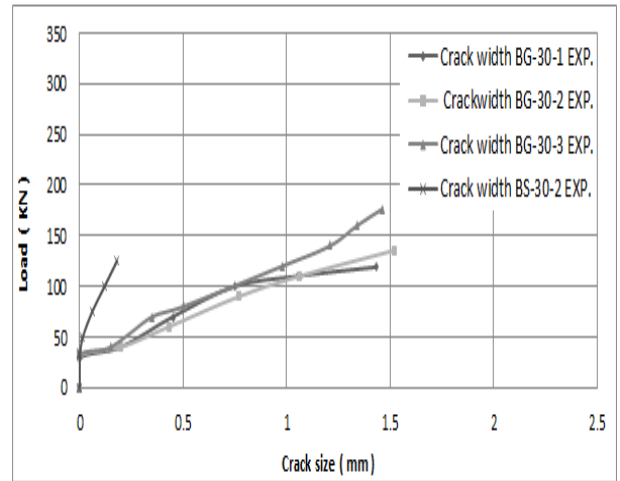


Figure 10. Load-crack size of beams with $f'_c=30$ MPa

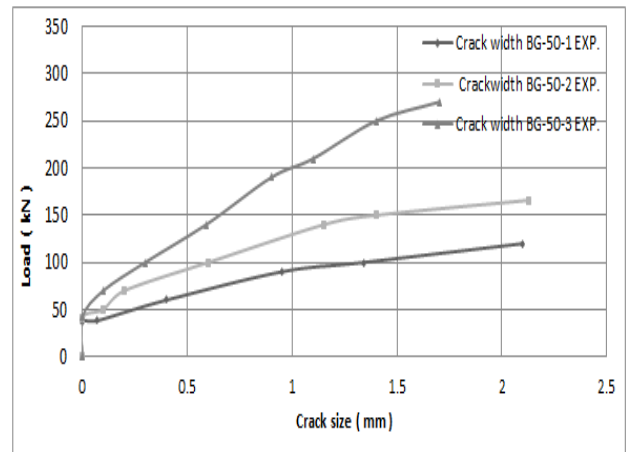


Figure 11. Load-crack size of beams with $f'_c=50$ MPa

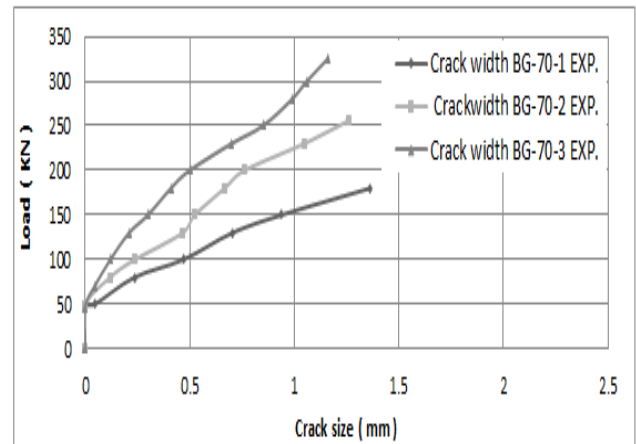


Figure 12. Load-crack size of beams with $f'_c=70$ MPa

4.5 Cracks number

Table 6 shows the cracks number that appear in the test span for all tested beams, results showed that a higher GFRP reinforcement ratio given a higher number of cracks and slower speed for cracks depth and size growing, at the same load value, a lesser crack size was obtained when a higher GFRP reinforcement ratio was used. In addition for beams with the same reinforcement area BG-30-2 and BG-70-1, increasing the concrete compressive strength from 30 to 70 MPa decreased number of cracks at service and ultimate loads.

4.6 Comparison between GFRP and steel reinforcement

Table 7 shows the different of experimental results of BG-30-2 and BS-30-2 were reinforced by the same bars numbers and diameter and same concrete compressive strength but with different type of materials the first by GFRP and the second by steel bars. Results showed that the failure load for BG-30-2 was higher than BS-30-2 by 8.4%, while deflection, bar's strain and crack size at failure for BG-30-2 were higher BS-30-2 by 117.5, 240 and 740%, respectively

Table 6. Cracks numbers

Beam specimen	Reinforcements Ratio (%)	Service load P_s (kN) _a	Number of crack at P_s	W_{cr} at P_s (mm)	Number of crack at P_u	Maximum W_{cr} (mm)
BG-30-1	0.00383 ^b	65.7	2	0.61	5	1.43
BG-30-2	0.00529 ^c	74.5	4	0.53	8	1.4
BG-30-3	0.00984 ^d	114.4	5	0.44	10	1.36
BG-50-1	0.00433 ^b	66	2	0.67	5	2.1
BG-50-2	0.00767 ^c	91.3	2	0.6	8	2.0
BG-50-3	0.0136 ^d	175.5	4	0.5	11	1.7
BG-70-1	0.00529 ^b	99	1	0.6	3	1.35
BG-70-2	0.012 ^c	140.8	1	0.6	8	1.26
BG-70-3	0.01797 ^d	211.2	2	0.57	10	1.16

^a According to ACI440.1R-15 $P_s=0.55 P_u$ for $\rho_f \leq \rho_{fb}$
 $P_s=0.65 P_u$ for $\rho_f > \rho_{fb}$

^b Minimum reinforcement ratio (ρ_{fmin})

^c Balanced reinforcement ratio (ρ_{fb})

^d ($1.5 \rho_{fb}$)

Table 7. Comparison of experimental results of GFRP and steel reinforcement

Beam specimen	Reinforcement ratio (%)	Reinforcement type	Failure load, P_u (kN)	Ultimate deflection (mm)	Ultimate strain	Ultimate crack size (mm)
BG-30-2	0.00529	GFRP	135.5	2.35	0.0119	1.52
BS-30-2	0.00529	Steel	125	1.08	0.0035	0.18

5. Theoretical Calculation

In this study, the theoretical ultimate load P_u of GFRP reinforced beams were calculated according to the formulas supplied by ACI 440.1R-15 [25], CSA S806-12 [26] to verify the validity of these formulas to find the ultimate loads for continuous beams reinforced by GFRP bars.

5.1 Comparison of experimental with calculated ultimate load.

According to ACI 440.1R-15[25], the flexural strength of the FRP-reinforced concrete beam can be computed on the basis of strain compatibility, internal force balance and failure mode control (tension or compression failure). The expected failure modes can be found by comparing the actual reinforcement ratio ρ_f (Eq. (1)) to the balanced reinforcement ratio ρ_{fb} (Eq. (2)) which specifies the level of concrete crushing and FRP rupture.

$$\rho_f = \frac{A_f}{b \cdot d} \quad (1)$$

Where A_f is the area of the FRP bar, b is the size of the rectangular cross-section and d is the distance measured from the extreme compression fiber to the centroid of FRP bars.

$$\rho_{fb} = \alpha_1 \beta_1 \frac{f'_c}{f_{fu}} \frac{E_f \epsilon_{cu}}{E_f \epsilon_{cu} + f_{fu}} \quad (2)$$

Where f'_c is the concrete compressive strength, f_{fu} is the ultimate FRP bars tensile stress, E_f is the elastic modulus of the FRP, α_1 is the ratio of average stress of equivalent rectangular stress block to f'_c and ϵ_{cu} is the ultimate concrete strain equal to 3%. Factor β_1 can be found as follows:

$$\beta_1 = 0.85 - 0.05 \left(\frac{f'_c - 28}{7} \right) \geq 0.65 \quad (3)$$

- If $\rho_f < \rho_{fb}$ then the beam is considered to be under-reinforced, where the control limit is the rupture of the FRP bars, and M_n can be calculated as follows:

$$M_{n,ACI} = A_f f_{fu} \left(d - \frac{\beta_1 \times c}{2} \right) \quad (4)$$

Where c is the distance measured from the extreme compression fiber to the N.A.

- If $\rho_f > \rho_{fb}$, then the beam is considered over-reinforced, the control limit is the crushing of concrete, and the flexural strength M_n can be calculated as follows:

$$M_{n,ACI} = \rho_f f_f b d^2 \left(1 - 0.59 \rho_f \frac{f_f}{f'_c} \right) \quad (5)$$

Where f_f is the FRP bars tensile strength, which can be found as follows:

$$f_f = \left[\sqrt{\frac{(E_f \epsilon_{cu})^2}{4} + \frac{0.85 \beta_1 f'_c}{\rho_f} E_f \epsilon_{cu}} - 0.5 E_f \epsilon_{cu} \right] \leq f_{fu} \quad (6)$$

According to CSA S806-12 [26], the flexural strength of the FRP-reinforced concrete beam can be also computed on the basis of strain compatibility and internal force balance, but with ultimate concrete strain equal to 3.5%. The balanced reinforcement ratio can be computed as follows:

$$\rho_{fb} = \alpha_1 \beta_1 \frac{f'_c}{f_{fu}} \frac{E_f \epsilon_{cu}}{E_f \epsilon_{cu} + f_{fu}} \quad (7)$$

$$\alpha_1 = 0.85 - 0.0015 f'_c \geq 0.67 \quad (8)$$

$$\beta_1 = 0.97 - 0.0025 f'_c \geq 0. \quad (9)$$

- If $\rho_f < \rho_{fb}$ then the beam is failed by rupture of FRP bars, the section is said to be under-reinforced, and M_n can be calculated as follows:

$$M_{n,CAS} = \rho_f f_{fu} b d^2 \left(1 - \frac{\rho_f f_{fu}}{2 \alpha_1 f'_c} \right) \quad (10)$$

- If $\rho_f > \rho_{fb}$, then the beam is failed by crushing of concrete without rupture of the reinforcement, the section is said to be over-reinforced, and the flexural strength M_n can be calculated as follows:

$$M_{n,CAS} = \rho_f f_f b d^2 \left(1 - \frac{\rho_f f_f}{2 \alpha_1 f'_c} \right) \quad (11)$$

$$f_f = 0.5 E_f \varepsilon_{cu} \left[\left(1 + \frac{4\alpha_1 \beta_1 f_c}{\rho_f E_f \varepsilon_{cu}} \right)^{0.5} - 1 \right] \quad (12)$$

Table 8 shows the experimental and calculated results of ultimate load, the calculation equations given by ACI 440.1R-15 [25] and CSA S806-12 [26] showed good agreement of the flexural strength of beams by 98% and 95%, respectively."

measured from extreme tension fiber to the center of the closest level of longitudinal bars, and S is the bar spacing. As shown in Table 3, the accurateness of evaluation is highly reliant on the value of k_b , and the approximation is on the conservative side when $k_b = 1.4$.

CEB-FIP [29] model predicts the crack size as follows:

Table 8. Comparison of experimental and calculated ultimate loads

Beam specimen	$P_{u,exp}$ (kN)	$P_{u,ACI}$ (kN)	$P_{u,CAS}$ (kN)	$\frac{P_{u,exp}}{P_{u,ACI}}$	$\frac{P_{u,exp}}{P_{u,CAS}}$
BG-30-1	119.5	108	110.2	1.08	1.09
BG-30-2	135.5	137.3	136	0.99	1
BG-30-3	176	181.5	170	0.97	1.04
BG-50-1	125	114	115.8	1.1	1.08
BG-50-2	166	183.8	183	0.9	0.9
BG-50-3	270	254.8	240	1.06	1.14
BG-70-1	180	139.5	140	1.3	1.3
BG-70-2	256	275	270	0.93	0.95
BG-70-3	325	337.8	319.6	0.96	1.02
Mean				1.03	1.06

5.2 Comparison of experimental and calculated crack size

The ACI 440.1R-06 [9] mentions the next formula to compute the size of crack of member reinforced by FRP bars :

$$W = 2 \frac{f_f}{E_f} \beta K_b \sqrt{d_c^2 + \frac{S^2}{4}} \quad (13)$$

where W is the crack size at tensile face of the beam, f_f is the stress in the FRP reinforcement, E_f is the modulus of elasticity for the FRP reinforcement, β is the coefficient to contrary crack size corresponding to the level of reinforcement to the tensile face of beam, k_b is the coefficient that accounts for the degree of bond between the FRP bar and the surrounding concrete, ACI 440.1R-06 [9] suggests 1.4 for deformed FRP bars if k_b is not experimentally known, d_c is the thickness of concrete cover

$$W = \beta S_m \varepsilon_m \quad (14)$$

Where $\beta = 1.3$, S_m is the average crack spacing of the FRP reinforced member, ε_m is the mean reinforcement strain permitting for tension stiffening.

$$\varepsilon_m = \sigma_s [1 - \beta_1 \beta_2 (\sigma_{sr} / \sigma_s)^2] / E_f \quad (15)$$

σ_s is the stress in the tension reinforcement calculated on the base of a cracked section. σ_{sr} is the stress in the tension reinforcement calculated on the basis of a cracked section under loading circumstances that cause the first crack, $\beta_1 = 1.0$ for high-bond bars and 0.5 for plain bars; $\beta_2 = 1.0$ for single short-term loading and 0.5 for sustained or cyclic loading. ISIS Canada- 07[30] suggest the following equation for crack size calculation:

$$W = 2.2k_b \frac{f_f h_2}{E_f h_1} \sqrt[3]{d_c A} \quad (16)$$

Where k_b bond dependent coefficient. For FRP bars having bond properties similar to concrete, $k_b=1.0$, h_2 distance from the extreme tension surface to the N.A., h_1 distance from the centroid of tension reinforcement to the N.A. and A effective tension area of concrete surrounding the flexural tension reinforcement and having the same centroid as that reinforcement, divided by the number of bars. Table 9 shows the experimental and calculated crack size for all tested beams. The calculations of the ACI 440 formula show lowly agreement with the experimental results. The exactness of the formula mainly based on the value of k_b .

Most of the experimental data can be enclosed between $k_b = 1.0$ and $k_b = 1.4$. Following the ACI 440's recommendations, k_b of 1.4 can be used to evaluation the crack size, and it is on the conservative side. On the other hand the ISIS-Canada model's exactness is similarly dependent on the reinforcement ratio. For this study, ISIS-Canada model can calculate the crack size objectively well for the GFRP reinforced members. ISIS-Canada model is established based on the steel reinforced members, which usually have same (ρ_f) in this study. While CEB-FIP equations showed good agreement with experimental results for beams having concrete compressive strength 30 and 50 MPa, but results were less consistent with the beams with strength of 70 MPa.

Table 9. Experimental and calculated crack size

Beam specimen	W_{exp} (mm)	W_{ACI} (mm)	$W_{CEB-FIP}$ (mm)	W_{ISIS} (mm)
BG-30-1	1.43	1.28	1.38	1.43
BG-30-2	1.52	1.4	1.49	1.55
BG-30-3	1.46	1.34	1.55	1.45
BG-50-1	2.1	2.35	2.17	2
BG-50-2	2.13	2.27	2.08	1.99
BG-50-3	1.7	1.9	1.82	1.36
BG-70-1	1.36	1.86	1.6	1.6
BG-70-2	1.26	2.17	1.85	1.5
BG-70-3	1.16	1.37	1.3	1.21

6. Conclusion

This research analyzed the flexural efficiency of continuous concrete beams reinforced with (GFRP) bars. Evaluation of the experimental findings with the results determined using some codes formulas produced the following conclusions within the framework of this investigation and consideration of the materials used:

1. Increasing the reinforcement ratio from (ρ_{fmin}) to (ρ_{fb}), leads to increase the ultimate capacity by (13, 32 and 42) %, for beams with f'_c (30, 50 and 70 Mpa), respectively. While increasing (ρ_f) ratio from (ρ_{fb}) to (1.5 ρ_{fb}), however, leads to increase (P_u) by (30, 62.7 and 27%), for beams with f'_c (30, 50 and 70 Mpa), respectively.
2. The curves of load-deflection for beams with (GFRP) bars contain three parts; the performance of the un-cracked beams reflects the first part of the curve up to crack. The second part reflects the output of the cracked beams with reduced rigidity including a steep linear division that relates to the cracked beam response; and a nonlinear section after the beam.
3. Increasing (ρ_f) shows a major decrease in deflection at all loading stages.
4. GFRP bars reinforced continuous beams with collapsed by crushing of concrete, meanwhile they were over-reinforced designed, whereas the under-reinforced beam failed by rupture of GFRP bars.
5. At same load level the strain in GFRP bars decreased with increasing in (ρ_f), when the reinforcement ratio increased from (ρ_{fmin}) to (1.5 ρ_{fb}) GFRP bars strain decreased by (53, 72 and 78%) for beams with f'_c (30, 50 and 70 Mpa), respectively.
6. The position of the neutral axis (N.A) depth of the critical sections increases with the increase of the ratio of longitudinal reinforcement ratio from (ρ_{fmin}) to (1.5 ρ_{fb}) for all tested beams.
7. The cracks size was significantly decreased with increasing in reinforcement ratio, at the same load level increases in reinforcement ratio from (ρ_{fmin}) to (1.5 ρ_{fb}) decreasing the crack size by (30.2, 76.9 and 68%) for beams with f'_c (30, 50 and 70 Mpa), respectively.
8. The beam specimens with the same GFRP reinforcement area but differs only in compressive strength, BG-30-2 and BG-70-1, increasing the concrete compressive strength from 31.5 to 71.5 MPa reduced the deflection in the same consequent load levels, also first crack and ultimate load increased by (55.6 and 32.8 %), respectively, decreased the GFRP strain and crack size by (32.4 and 48.6%), respectively and decreased number of cracks at service and ultimate loads.
9. The effect of reinforcement type of BG-30-2 and BS-30-2 were reinforced by the same bars numbers and diameter and same concrete compressive strength but the first reinforced by GFRP and the second by steel bars. Results showed that the failure load for BG-30-2 was higher than BS-30-2 by 8.4%, while deflection, bar's strain and crack size at failure for BG-30-2 were higher BS-30-2 by 117.5, 240 and 740%, respectively.
10. The formulas given by ACI440.1R-15 and CSA S806-12 showed good estimation of ultimate load of continuous beams reinforced by GFRP bars.
11. ISIS-Canada equation can calculate the size of crack objectively well for the members reinforced with GFRP bars, however the calculations of the ACI 440 formula give lowly agreement with the experimental results.

Conflict of interest

There are not conflicts to declare.

7. References

1. Bakis, C. E., Bank, L. C., Brown, V., Cosenza, E., Davalos, J. F., Lesko, J. J., ... & Triantafillou, T. C. (2002). Fiber-reinforced polymer composites for construction—State-of-the-art review. *Journal of composites for construction*, 6(2), 73-87..
2. Correia, J. R., Cabral-Fonseca, S., Branco, F. A., Ferreira, J. G., Eusébio, M. I., & Rodrigues, M. P. (2006). Durability of pultruded glass-fiber-reinforced polyester profiles for structural applications. *Mechanics of Composite Materials*, 42(4), 325-338..
3. Bai, Y., Post, N. L., Lesko, J. J., & Keller, T. (2008). Experimental investigations on temperature-dependent thermo-physical and mechanical properties of pultruded GFRP composites. *Thermochimica Acta*, 469(1-2), 28-35..
4. Fico, R. (2007). Limit states design of concrete structures reinforced with FRP bars. University of Naples Federico II, PH. D. Thesis..
5. Keller, T. (2001). Recent all-composite and hybrid fibre-reinforced polymer bridges and buildings. *Progress in Structural Engineering and Materials*, 3(2), 132-140..
6. Keller, T. (1999). Towards structural forms for composite fibre materials. *Structural engineering international*, 9(4), 297-300..
7. Sobrino, J. A., & Pulido, M. D. G. (2002). Towards advanced composite material footbridges. *Structural engineering international*, 12(2), 84-86..
8. Barris, C., Torres, L., Turon, A., Baena, M., & Catalan, A. (2009). An experimental study of the flexural behaviour of GFRP RC beams and comparison with prediction models. *Composite Structures*, 91(3), 286-295..
9. ACI 440.1 R-06, (2006.). "Guide for the design and construction of structural concrete reinforced with FRP bars". American Concrete Institute.
10. Yinghao, L., & Yong, Y. (2013). Arrangement of hybrid rebars on flexural behavior of HSC beams. *Composites Part B: Engineering*, 45(1), 22-31..
11. Adam, M. A., Said, M., Mahmoud, A. A., & Shanour, A. S. (2015). Analytical and experimental flexural behavior of concrete beams reinforced with glass fiber reinforced polymers bars. *Construction and Building Materials*, 84, 354-366..
12. Maranan, G. B., Manalo, A. C., Benmokrane, B., Karunasena, W., & Mendis, P. (2015). Evaluation of the flexural strength and serviceability of geopolymer concrete beams reinforced with glass-fibre-reinforced polymer (GFRP) bars. *Engineering Structures*, 101, 529-541..
13. Yang WR, He XJ, Dai L. (2017 Feb)." Damage behavior of concrete beams reinforced with GFRP bars". *Composite Structures*. 1;161:173-86.
14. Dong, H. L., Zhou, W., & Wang, Z. (2019). Flexural performance of concrete beams reinforced with FRP bars grouted in corrugated sleeves. *Composite Structures*, 215, 49-59..
15. Ahmed, H. Q., Jaf, D. K., & Yaseen, S. A. (2020). Flexural strength and failure of geopolymer concrete beams reinforced with carbon fibre-reinforced polymer bars. *Construction and Building Materials*, 231, 117185. 20;231:117185.
16. Tezuka M, Ochiai M, Tottori S, Sato R. 1995. "Experimental study on moment redistribution of continuous beams reinforced or pretensioned with fiber

- reinforced plastic". In RILEM PROCEEDINGS (pp. 387-387). CHAPMAN & HALL.
17. Grace NF, Soliman AK, Abdel-Sayed G, Saleh KR. 1998 Nov. "Behavior and ductility of simple and continuous FRP reinforced beams". *Journal of composites for construction*;2(4):186-94.
 18. Habeeb, M. N., & Ashour, A. F. (2008). Flexural behavior of continuous GFRP reinforced concrete beams. *Journal of composites for construction*, 12(2), 115-124..
 19. Zinkaah, O. H., & Ashour, A. (2019, June). Load capacity predictions of continuous concrete deep beams reinforced with GFRP bars. In *Structures* (Vol. 19, pp. 449-462). Elsevier..
 20. Mohamed, A. M., Mahmoud, K., & El-Salakawy, E. F. (2020). Behavior of Simply Supported and Continuous Concrete Deep Beams Reinforced with GFRP Bars. *Journal of Composites for Construction*, 24(4), 04020032..
 21. ACI 318R-14.(2014)." Building code requirements for structural concrete (ACI 318-14) and commentary ".American Concrete Institute. 1–519. Detroit.
 22. Abdallah, M., Al Mahmoud, F., Khelil, A., Mercier, J., & Almassri, B. (2020). Assessment of the flexural behavior of continuous RC beams strengthening with NSM-FRP bars, Experimental and analytical study. *Composite Structures*, 112127..
 23. NANJING FINGHUI ® _China: producer of composite reinforcing elements for design and construction. China.
 24. ASTM, Designation: D 7205–06. (2006)." Standard Test Method for Tensile Properties of Fiber Reinforced Polymer Matrix Composite Bars",.
 25. ACI 440.1R-15,.(2015)."Guide for the design and construction of Concrete Reinforced with Fiber Reinforced Polymers (FRP) bars", ACI Committee 440, American Concrete Institute, Farmington Hills, MI, USA,.
 26. CSA S806-12.(2012). "Design and construction of building structures with fiber-reinforced polymers".. Mississauga, Ontario, Canada: Canadian Standards Association.
 27. GangaRao, H. V., Taly, N., & Vijay, P. V. (2006). Reinforced concrete design with FRP composites. CRC press..
 28. Kakizawa, T., Ohno, S., & Yonezawa, T. (1993). Flexural behavior and energy absorption of carbon FRP reinforced concrete beams. *Special Publication*, 138, 585-598..
 29. CEB-FIP.(2007)." FRP reinforcement in RC structures". *Fib bulletin* 40. International Federation for Structural Concrete (fib);.
 30. ISIS, D. M. N. (2007). 3: Reinforcing Concrete Structures with Fibre Reinforced Polymers. *Intelligent Sensing for Innovative Structures Canada*, 449-458..